

Modeling of performance and thermodynamic study of a gas turbine power plant

Mohamed Elwardany^{1,*}, A. M. Nassib¹, Hany A. Mohamed^{1,2}, M. R. Abdelaal²

¹ Department of Mechanical Power Engineering, Faculty of Engineering, Assiut University, Assiut 71516, Egypt

² Manufacturing Department, Modern Academy for Engineering and Technology, Cairo 11571, Egypt

* Corresponding author: Mohamed Elwardany, M.Wardany@anu.edu.eg

CITATION

Elwardany M, Nassib AM, Mohamed HA, Abdelaal MR. Modeling of performance and thermodynamic study of a gas turbine power plant. *Thermal Science and Engineering*. 2024; 7(4): 8016. <https://doi.org/10.24294/tse.v7i4.8016>

ARTICLE INFO

Received: 16 June 2024

Accepted: 30 July 2024

Available online: 9 October 2024

COPYRIGHT



Copyright © 2024 by author(s).

Thermal Science and Engineering is published by EnPress Publisher, LLC. This work is licensed under the Creative Commons Attribution (CC BY) license.

<https://creativecommons.org/licenses/by/4.0/>

Abstract: The efficiencies and performance of gas turbine cycles are highly dependent on parameters such as the turbine inlet temperature (TIT), compressor inlet temperature (T1), and pressure ratio (R_c). This study analyzed the effects of these parameters on the energy efficiency, exergy efficiency, and specific fuel consumption (SFC) of a simple gas turbine cycle. The analysis found that increasing the TIT leads to higher efficiencies and lower SFC, while increasing the T_o or R_c results in lower efficiencies and higher SFC. For a TIT of 1400 °C, T1 of 20 °C, and R_c of 8, the energy and exergy efficiencies were 32.75% and 30.9%, respectively, with an SFC of 187.9 g/kWh. However, for a TIT of 900 °C, T1 of 30 °C, and R_c of 30, the energy and exergy efficiencies dropped to 13.18% and 12.44%, respectively, while the SFC increased to 570.3 g/kWh. The results show that there are optimal combinations of TIT, T_o , and R_c that maximize performance for a given application. Designers must consider trade-offs between efficiency, emissions, cost, and other factors to optimize gas turbine cycles. Overall, this study provides data and insights to improve the design and operation of simple gas turbine cycles.

Keywords: gas turbine; thermal analysis; energy; exergy; efficiency

1. Introduction

Energy consumption is a key indicator of development, with population growth, urbanization, industrialization, and technological progress driving increased energy use. However, this rapid rise has contributed to pollution and the greenhouse effect. Currently, 80% of electricity is generated from fossil fuels, while renewable sources provide 20% [1–4]. Global electricity demand is growing by approximately 6% annually [5], and fossil fuels remain a major source of CO₂ emissions [6–12]. Natural gas (NG) accounts for 22% of global energy production, and demand for NG is expected to rise by 2.7% annually. By 2040, NG is projected to produce 28% of global electricity, up from 22% in 2012 [13–17]. The term “thermal power plant analysis” encompasses the efficient use of energy resources. Before 1940, efficiency was assessed using the first law of thermodynamics [18–23], while the second law, or exergy analysis, identifies where and why energy losses occur. This method is crucial for detecting inefficiencies and optimizing power plant performance [16,24–33].

Gas turbines are widely used in power generation due to their flexibility, efficiency, and ability to provide both baseload and peak-load power. Advances in materials and cooling technologies have significantly improved their thermal efficiency, making them a preferred choice for modern power plants. One of the primary challenges in gas turbine operation is managing the high temperatures within the combustion chamber, which directly affects the turbine’s performance and

longevity. Research has focused on optimizing turbine blade materials, cooling techniques, and combustion processes to enhance both the energy and exergy efficiencies of gas turbines. Combined cycle power plants (CCPPs), which integrate gas and steam turbines, have become increasingly popular for their ability to achieve higher overall efficiencies by utilizing waste heat from the gas turbine to power the steam cycle [34–37]. The thermodynamic simple gas turbine cycle employs a gas turbine to transform gas energy into mechanical work. The compressor, combustion chamber, and turbine comprise the gas turbine. Before being burned in the combustion chamber, the compressor compresses air. The turbine blades move when hot combustion gases expand across them. The turbine releases exhaust gas. Gas turbines have combustor, compressor, and power turbine units. To power an open-cycle gas turbine, centrifugal or axial flow compressors compress ambient air. Air is compressed by the compressor. Fuel and pressurized air enter the combustion chamber. Gases power the turbine. The combination ignites to generate velocity gas. When turbine blades spin, the generator's rotor shaft revolves. Energy from turning the turbine shaft may power industrial machines and create electricity [6,38,49]. Ibrahim et al. [40] conducted an analysis of a simple gas turbine model using energy and exergy assessments. Their findings indicated that the combustion chamber was responsible for the highest exergy destruction. The air compressor demonstrated energy and exergy efficiencies of 92% and 94.9%, respectively, while the combustion chamber showed efficiencies of 61.8% and 67.5%. In comparison, the gas turbine achieved energy and exergy efficiencies of 82% and 92%. Overall, the system's energy and exergy efficiencies were reported as 34.3% and 32.4%, respectively.

The impacts of several operational parameters of gas turbine power plants were studied by Kurt et al. [41]. Results demonstrated that the overall power output reaches its maximum according to the TIT at $P_R = 22$, TIT = 1600 K, and CIT = 288.15 K. In contrast, it reaches its maximum according to the CIT at $P_R = 18$ and CIT = 273.15 K, and TIT = 1423.15 K. De Sa and Al Zubaidy [42] suggested an empirical relation between the capacity of the gas turbine to produce electricity when subjected to ambient air conditions that differ from ISO conditions. With data readings exceeding 8000 for gas turbine operation around 280 days, results showed that the gas turbine lost 1.47 MW of power output and 0.1% of thermal efficiency for every degree increase in ambient temperature over ISO conditions. Abou Al-Sood et al. [43] analyzed the performance of a gas turbine cycle featuring an irreversible intercooler, regenerative system, and reheat cycle. The results indicated that the minimum temperature ranged from 302 K to 315 K, while the maximum temperature was between 1320 K and 1360 K. The optimal pressure for the cycle was found to lie between 1449 kPa and 2830 kPa to optimize all performance parameters. Salah et al. [44] examined the influence of ambient temperature, compression ratio, and relative humidity on the thermal and exergy performance of a gas power plant over a full year under real weather conditions. Using ChemCad simulations, they identified system inefficiencies and losses, with the combustion chamber causing the most significant exergy destruction, followed by the compressor and gas turbine. Their findings showed that energy efficiency peaked at 37% in November, when the ambient temperature was 19.39 °C. Additionally, specific fuel consumption (SFC) increased with higher ambient temperatures, reaching its peak at 33.27 °C.

In this study, we will evaluate the performance of a gas turbine cycle using energy and exergy analysis. The objective is to examine the effects of design parameters on gas turbine performance, with simulations assessing how environmental conditions and other key factors impact the cycle. The research aims to identify optimal design parameters for gas turbine power plants, utilizing EES software to model cycle performance based on operational data from previous studies.

2. Modelling and analysis

In this study, a thermodynamic analysis of simple gas turbine (SGT) cycles is performed using conventional energy and exergy analysis to assess cycle performance. As shown in **Figure 1**, the SGT process involves compressing air in the compressor, mixing it with fuel, and igniting it in the combustion chamber. The resulting high-temperature exhaust gases expand through the turbine, producing mechanical work, after which they are released. This energy can be harnessed for electricity generation and powering industrial equipment.

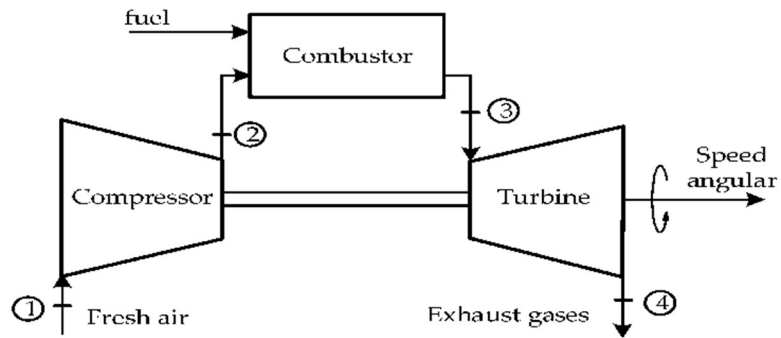


Figure 1. Simple gas turbine (SGT).

Table 1. Thermodynamic assumptions used for the (SGT) model based on [28,29].

Data	Value
Dead state conditions	$P_0 = 1.01 \text{ bar}, T_0 = 293.15 \text{ K}$
Turbine isentropic efficiency	87%
Compressor isentropic efficiency	85%
combustion efficiency	0.98 %
Ambient temperature	298 k
Compressor inlet pressure	94 kPa
Specific heat of air	1.005 kJ/kg K
Specific heat of gasses	1.14 kJ/kg K
Ratio of specific heat for gasses	1.33
Ratio of specific heat for air	1.4
Fuel type	NG

Energy analysis, based on the first law of thermodynamics, and exergy analysis, grounded in the second law, are employed to evaluate the cycle's efficiency. The analysis includes several assumptions, summarized in **Table 1**.

2.1. Energy analysis

The energy assessment of a gas turbine cycle is based on the Brayton cycle, involving calculations of the system's energy input and output. The key components include the air compressor, combustion chamber, and gas turbine. The following equations are used to analyze each part of the cycle [45]. Compressor:

$$T_2 = T_1 \left(1 + \frac{1}{\eta_{AC}} \left(r_{AC}^{\frac{k-1}{k}} - 1 \right) \right) \quad (1)$$

$$\dot{W}_{AC} = \dot{m}_a c_{pa} (T_2 - T_1) \quad (2)$$

$$c_{pa}(T) = 1.048 - \left(\frac{1.83T}{10^4} \right) + \left(\frac{9.45T^2}{10^7} \right) - \left(\frac{5.49T^3}{10^{10}} \right) + \left(\frac{7.92T^4}{10^{14}} \right) \quad (3)$$

In Equation (1), T_1 and T_2 denote the air temperatures at the compressor inlet and outlet, respectively, while k is the specific heat ratio and r is the compression ratio. The compressor's power consumption is determined using Equation (2), and Equation (3) defines the specific heat of air as a function of temperature.

Combustion chamber:

$$\dot{m}_a h_2 + \dot{m}_f \text{LHV} = \dot{m}_g h_3 + (1 - \eta_{cC}) \dot{m}_f \text{LHV} \quad (4)$$

$$\dot{m}_g = \dot{m}_f + \dot{m}_a \quad (5)$$

$$f = \frac{\dot{m}_f}{\dot{m}_a} = \frac{C_{pg} \times T_3 - C_{pa} T_2}{\text{LHV} - C_{pg} \times T_3} \quad (6)$$

The lower heating value (LHV) varies depending on the fuel's properties. In this analysis, natural gas is utilized in the combustion chamber.

Gas turbine:

$$T_4 = T_3 \left(1 - \eta_{GT} \left(1 - \left(\frac{P_3}{P_4} \right)^{\frac{k-1}{k}} \right) \right) \quad (7)$$

$$\dot{W}_{GT} = \dot{m}_g c_{p,g} (T_{A_3} - T_{A_4}) \quad (8)$$

$$C_{pg}(T) = 0.991 + \left(\frac{6.997T}{10^5} \right) + \left(\frac{2.712T^2}{10^7} \right) - \left(\frac{1.2244T^3}{10^{10}} \right) \quad (9)$$

In Equation (7), T_3 and T_4 denote the turbine's inlet and outlet combustion gas temperatures, respectively. The turbine's power output is determined using Equation (8), while Equation (3) calculates the air's specific heat as a function of temperature.

2.2. Exergy analysis

Exergy represents the maximum useful work a system can perform as it moves toward equilibrium with its environment. Based on the second law of thermodynamics and applying mass and energy balances, exergy analysis provides a powerful method for assessing energy system performance. Exergy consists of four parts: chemical, physical, kinetic, and potential. However, in typical analyses, only chemical and physical exergies are considered, while kinetic and potential components are often neglected. Physical exergy refers to a system's ability to perform work, while chemical exergy is tied to differences in chemical composition from equilibrium conditions [46]. The general equations for exergy analysis are presented below.

$$\dot{E}_{x,\text{heat}} + \sum_i \dot{m}_i e_{x,i} = \sum_e \dot{m}_e e_{x,e} + \dot{E}_{x,w} + \dot{I}_{\text{dest}} \quad (10)$$

$$\dot{E}_{x,w} = \dot{W} \quad (11)$$

$$\dot{E}_{x,\text{heat}} = \left(1 - \frac{T_o}{T_i}\right) \dot{Q}_i \quad (12)$$

$$\dot{E}_x = \dot{E}_{x,\text{phy}} + \dot{E}_{x,\text{che}} \quad (13)$$

By applying Equation (10), the exergy flow rate for each system component can be calculated. Equation (11) represents the system's work derived from the exergy flow. The exergy generation rate due to heat is expressed in Equation (12). Finally, Equation (13) outlines the physical and chemical exergies of the component [47].

Physical exergy:

The physical exergy arises from the system's deviation in pressure and temperature relative to its dead state [40]. The following equations can be used to compute the physical exergy of the system.

$$e_x = e_{x,\text{phy}} + e_{x,\text{che}} \quad (14)$$

$$e_{x,\text{phy}} = e_x^T + e_x^P \quad (15)$$

$$e_x^T = c_p \left((T - T_o) - T_o \ln \frac{T}{T_o} \right) \quad (16)$$

$$e_x^P = RT_o \ln \frac{P}{P_o} \quad (17)$$

The physical exergy can be calculated using Equation (15), with Equations (16) and (17) defining it in terms of temperature and pressure. In these equations, P_o and T_o represent the ambient pressure and temperature, while C_p and R denote the specific heat at constant pressure and the gas constant, respectively [47].

Chemical exergy:

Chemical exergy arises when the chemical composition of a system differs from the surrounding dead-state conditions [40]. The exergy flow of the fuel can be calculated using the following equation.

$$\xi = \frac{e_{x,\text{fuel}}}{\text{LHV}_{\text{fuel}}} \quad (19)$$

In Equation (19), ξ represents the ratio of exergy flow to the LHV of the fuel. ($\text{LHV}_{\text{fuel}} = 48,806 \text{ kJ/kg}$) Usually, the value for ξ is 1.06 for NG. The following equation can be used to determine the exergy of the combustion products [40].

$$e_{x,\text{cg}} = \frac{[\sum_{i=1}^n x_i e_{x,\text{che},i} + RT_o \sum_{x=i}^n x_i \ln(x_i)]}{\sum(x_i)} \quad (20)$$

In Equation (20), the subscript i refers to the type of air fraction, x is the molar fraction, and $e_{x,\text{ch}}$ represents the standard chemical exergy of each component. **Table 2** provides the standard chemical exergy and molar fraction of each gas. More accurate results can be obtained using the following equations [48].

$$\lambda = \frac{0.058 \dot{m}_{\text{air}}}{\dot{m}_{\text{fuel}}} \quad (21)$$

$$x_{\text{N}_2} = \frac{(7.524)\lambda}{1 + (9.6254)\lambda} \quad (22)$$

$$x_{O_2} = \frac{2(\lambda - 1)}{1 + (9.6254)\lambda} \quad (23)$$

$$x_{CO_2} = \frac{1 + (0.0028)\lambda}{1 + (9.6254)\lambda} \quad (24)$$

$$x_{H_2O} = \frac{2 + (0.0972)}{1 + (9.6254)\lambda} \quad (25)$$

Equations (21)–(25) can be used to calculate the molar fraction of each component in the combustion products, applicable specifically when natural gas (NG) is used as the fuel. In these equations, the subscript “*k*” denotes the fuel-air ratio [48].

Table 2. Standard exergy and molar fraction [32].

Element	$e_{x,che}$ (KJ/mol)	Molar fraction (%)
N ₂	0.72	75.67
O ₂	3.97	20.34
CO ₂	19.87	0.03
H ₂ O	9.49	3.03

Exergy efficiency is a crucial metric for evaluating how well a system utilizes energy. It is defined as the ratio of useful work output to the total energy input. A higher exergy efficiency indicates reduced energy wastage and enhanced productivity. This measure is essential for assessing both the long-term sustainability and economic feasibility of energy systems. To understand exergy destruction, the exergy flow rate for each component is calculated, revealing a decrease in exergy after each process.

Exergy destruction:

Exergy destruction is assessed by calculating the exergy flow rate for each component, which shows a decrease in exergy after each process. Typically, this destruction is quantified using Equation (27) [48].

$$\dot{E}_{x,in} - \dot{E}_{x,out} = \dot{E}_{x,D} \quad (26)$$

Air compressor:

$$\dot{E}_{x,D,AC} = \dot{E}_{x_1} - \dot{E}_{x_2} + \dot{W}_{AC} \quad (27)$$

Combustion chamber:

$$\dot{E}_{x,D,CC} = \dot{E}_{x_2} + \dot{E}_{x_5} - \dot{E}_{x_3} \dot{E}_{x,D,AC} = \dot{E}_{x_1} - \dot{E}_{x_2} + \dot{W}_{AC} \quad (28)$$

Gas turbine:

$$\dot{E}_{x,D,GT} = \dot{E}_{x_3} - \dot{E}_{x_4} - \dot{W}_{GT} \quad (29)$$

Systems efficiency:

Each component is evaluated for both energy and exergy to determine which has the highest and lowest efficiency. Exergy efficiency is calculated using the following equation [48].

Air compressor:

$$\eta_{x,AC} = \frac{\dot{E}_{x_2} - \dot{E}_{x_1}}{\dot{W}_{AC}} \quad (30)$$

Combustion chamber:

$$\eta_{x,CC} = \frac{\dot{E}_{x_3}}{\dot{E}_{x_3} - \dot{E}_{x_1}} \quad (31)$$

Gas turbine:

$$\eta_{x,GT} = \frac{\dot{W}_{GT}}{\dot{E}x_3 - \dot{E}x_4} \quad (32)$$

Equation (30) is used to calculate the efficiency of the air compressor, considering work output and exergy destruction. Similarly, Equation (32) assesses the efficiency of the gas turbine by considering its exergy destruction and work output. For the combustion chamber, Equation (31) evaluates efficiency based on the exergy rate and exergy destruction of the fuel [48]. The overall exergy and energy efficiencies of the simple gas turbine cycle can be determined using the equations provided below [47].

$$\dot{W}_{Net} = \dot{W}_{GT} - \dot{W}_{AC} \quad (33)$$

$$SFC = 3600 \frac{\dot{m}_{fuel}}{\dot{W}_{net}} \quad (34)$$

$$\eta_I = \frac{\dot{W}_{net}}{\dot{m}_{fuel}LHV} \quad (35)$$

$$\eta_{II} = \frac{\dot{W}_{net}}{\dot{E}x_f} \quad (36)$$

Equation (34) calculates the specific fuel consumption of the gas turbine. Equation (36) provides the overall exergy efficiency, with $\dot{E}x_f$ representing the fuel exergy flow rate. Equation (35) is used to determine the overall energy efficiency of the cycle [47].

2.3. Model validation

Based on the analysis, a simulation program was created using EES software for the SGT. The results were validated against those from [40]. **Table 3** presents the operating parameters used for validation, while **Figure 2** illustrates the comparison between the reference and current models, which shows strong agreement.

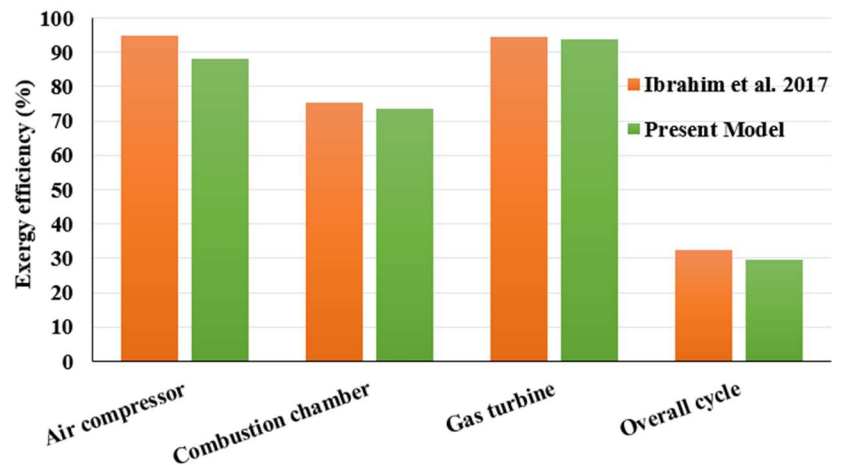


Figure 2. Comparison between the exergy efficiency for all components of simple gas cycle in the present model with [40].

Table 3. Operating parameters for validation model based on [40].

Parameters	Value
Ambient air temperature	18.34 °C
Inlet pressure	94 kPa
Air mass flow rate	439.802 kg/s
Fuel mass flow rate	10.473 kg/s
Compression ratio	15.64
Fuel type	NG

3. Results and discussion

This section details the simulation results regarding how operating conditions influence the performance of gas turbine cycles. Using a computer model developed in EES software, we analyzed the effects of various operating parameters on specific fuel consumption (SFC), energy, and exergy efficiencies. The cycle’s performance was evaluated across different operational scenarios. The findings are based on previously discussed theoretical relationships. The simulation results for the SGT cycle are presented and examined in this section.

3.1. Effect of compression ratio and turbine inlet temperature on energy and exergy efficiencies

Figure 3 provides performance data for a gas turbine under three different turbine inlet temperature (TIT) conditions (900 [c], 1200 [c], and 1400 [c]) at a constant ambient temperature of 25 [c]. The data in this table shows that increasing the TIT leads to higher gas turbine efficiencies, both in terms of energy and exergy efficiency. This suggests that higher pressure ratios can lead to more efficient energy conversion, even when the TIT is held constant. The data also shows that, for a given TIT, the exergy efficiency is lower than the energy efficiency. However, the difference between energy and exergy efficiencies decreases as the pressure ratio increases. However, it is worth noting that the rate of increase in efficiency with respect to pressure ratio is not constant across different TIT conditions, this indicates that the optimal pressure ratio for a given TIT may depend on the specific design and operating conditions of the gas turbine. Overall, this table provides additional insights into the performance of a gas turbine under different TIT and pressure ratio conditions, taking into account both idealized maximum efficiency and real-world losses and inefficiencies. However, additional factors such as the specific design and operating conditions of the gas turbine, as well as environmental and economic considerations, would need to be taken into account for a more thorough analysis.

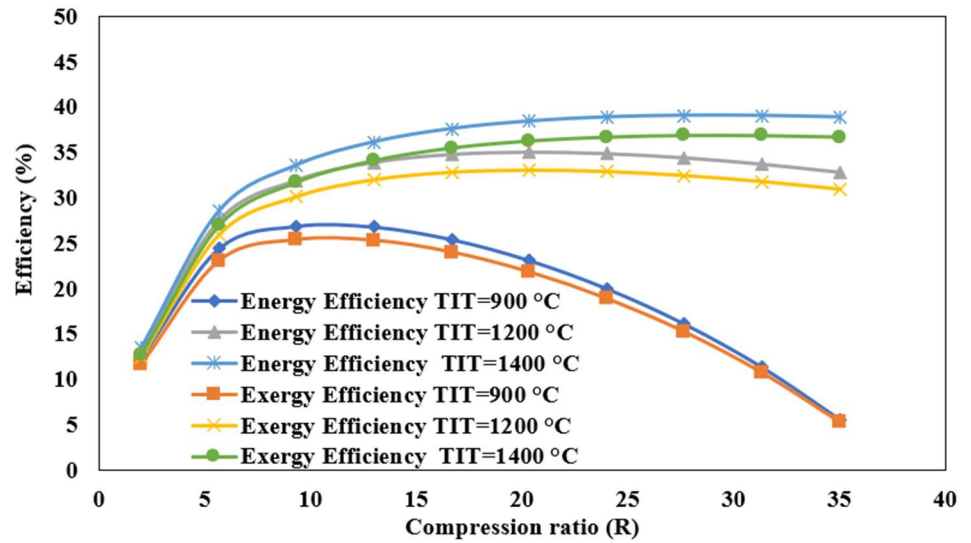


Figure 3. Illustrates how energy and exergy efficiencies vary with compression ratio and turbine inlet temperature.

3.2. Impact of ambient temperature and compression ratio on energy and exergy efficiency

Figure 4 shows the energy and exergy efficiencies of a gas turbine at different operating conditions. The data is presented in three sets, each with a constant value for the turbine inlet temperature (TIT) of 1400 °C and different values for the ambient air temperature (T_o) of 5 °C, 20 °C, and 35 °C. For example, at a TIT of 1400 °C and a T_o of 5 °C, the energy efficiency of the gas turbine is 13.65% at a compression ratio of 2, and the exergy efficiency is 12.88%. As the compression ratio increases, both the energy and exergy efficiencies of the gas turbine also increase. In general, a higher compression ratio can increase the energy and exergy efficiencies of a gas turbine. However, increasing the compression ratio can also increase the risk of engine knock and other undesirable effects, so there is often a trade-off between efficiency and other factors such as engine durability and emissions. By analyzing the data in the figure, it may be possible to identify the optimal operating conditions for the gas turbine to achieve the highest energy or exergy efficiency. For example, it may be possible to identify the compression ratio and ambient temperature that would result in the highest efficiency. Additionally, analyzing the data may also reveal areas where the design of the gas turbine could be improved to increase efficiency, such as by optimizing the combustion process or improving the design of the compressor and turbine components.

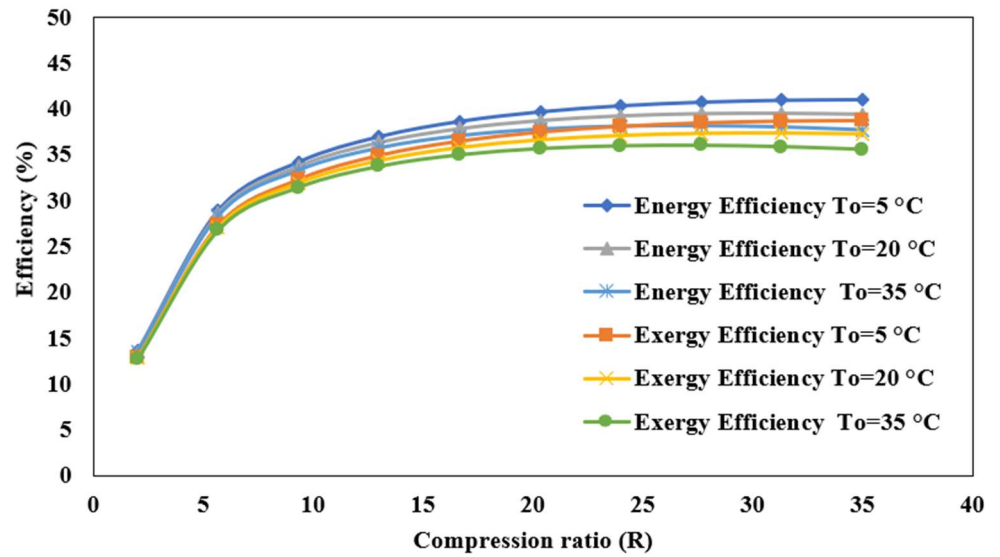


Figure 4. Illustrates how energy and exergy efficiencies vary with compression ratio and turbine ambient temperature.

3.3. Impact of turbine inlet temperature and ambient temperature on energy and exergy efficiencies

In gas turbine cycles, the turbine inlet temperature (TIT) and compressor inlet temperature (T_1) are two of the most important parameters that influence the performance of the system. **Figure 5** shows the energy and exergy efficiencies for gas turbine cycles operating at different compressor inlet temperatures (T_1) and a fixed pressure ratio ($R = 20$) for three different turbine inlet temperatures (TIT): 900 °C, 1200 °C, and 1400 °C. Based on the data in the figure, it can be observed that increasing the TIT generally results in higher energy and exergy efficiencies for a fixed compressor inlet temperature and pressure ratio. For example, comparing the values for $T_1 = 5$ °C and $R = 20$, the energy efficiency increases from 27.71% to 36.83% to 39.62%, as the TIT increases from 900 °C to 1200 °C to 1400 °C, respectively. It can also be seen that, at a fixed TIT, there is an optimum value for T_1 that maximizes the energy and exergy efficiencies. This optimal value of T_1 decreases as the TIT increases. For example, for TIT = 900 °C and $R = 20$, the maximum energy efficiency is achieved at $T_1 = 15$ °C, while for TIT = 1400 °C and $R = 20$, the maximum energy efficiency is achieved at $T_1 = 11.7$ °C. Higher TITs generally lead to higher efficiencies, but there are practical limitations to how high the TIT can be due to material and technology constraints. Similarly, lower T_o values can improve efficiency, but only up to a certain point, as lower temperatures can reduce the power output of the gas turbine. Overall, higher TITs generally lead to higher efficiencies, but there are practical limitations to how high the TIT can be due to material and technology constraints. Similarly, lower T_o values can improve efficiency, but only up to a certain point, as lower temperatures can reduce the power output of the gas turbine. The data in the figure can be used to optimize the design and operation of gas turbine cycles by selecting the values of TIT and T_1 that maximize the energy and exergy efficiencies. The optimal values depend on the specific application and operating conditions.

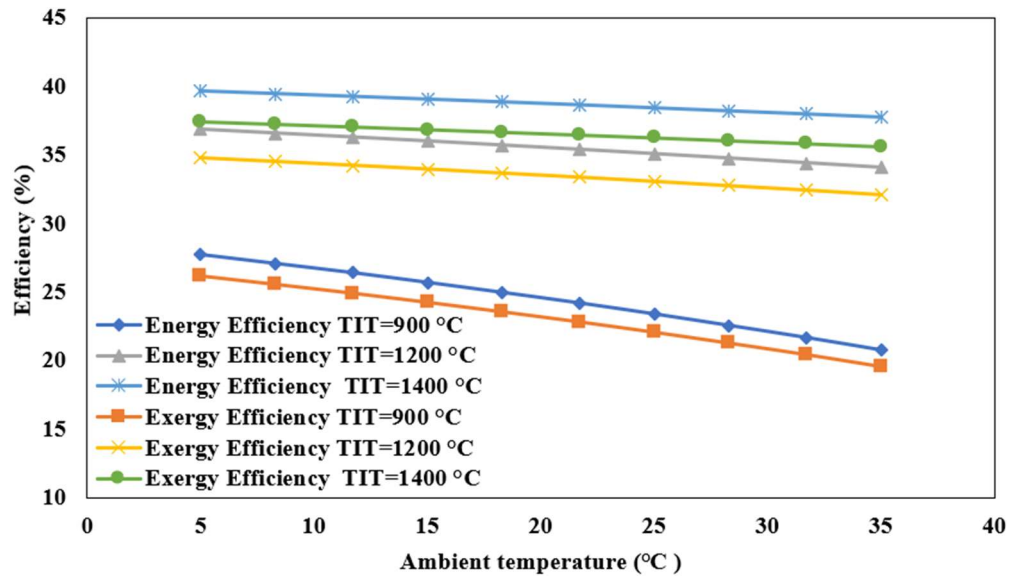


Figure 5. Illustrates how energy and exergy efficiencies vary with turbine ambient temperature and ambient temperature.

3.4. Impact of turbine inlet temperature and compression ratio on specific fuel consumption

The specific fuel consumption (SFC) is a key parameter for assessing the fuel efficiency of gas turbine cycles. It represents the amount of fuel consumed per unit of power output. The lower the SFC, the more efficient the gas turbine cycle is at converting fuel into usable power. The SFC is influenced by several factors, including the compressor and turbine efficiencies, the combustion process, the pressure ratio, and the turbine inlet temperature (TIT). Generally, higher pressure ratios and TITs result in lower SFC values, while lower SFC values can be achieved by improving the efficiency of the compressor and turbine or by optimizing the combustion process. In **Figure 6**, the SFC values are shown for gas turbine cycles operating at different pressure ratios and TITs with a fixed compressor inlet temperature of 25 °C. The data shows that increasing the TIT generally results in lower SFC values, as more of the energy in the fuel is converted into useful work. Similarly, increasing the pressure ratio can also improve fuel efficiency, as the higher pressure ratio leads to a higher turbine work output for the same amount of fuel input. For example, comparing the values for PR = 2, the SFC decreases from 520 g/kWh to 247.7 g/kWh to 214 g/kWh, as the TIT increases from 900 °C to 1200 °C to 1400 °C, respectively. It can also be seen that, at a fixed TIT, there is an optimal value for the pressure ratio that minimizes the SFC. This optimal value of PR generally increases as the TIT increases. For example, for TIT = 900 °C, the minimum SFC is achieved at PR = 16.67, while for TIT = 1400 °C, the minimum SFC is achieved at PR = 35. However, it's important to note that increasing the TIT and pressure ratio can also lead to higher operating temperatures and pressures, which can increase the risk of component failure and reduce the overall reliability of the system. Therefore, a trade-off must be made between fuel efficiency and reliability when designing and operating gas turbine cycles. In addition to the SFC, other factors such as emissions, cost, and performance requirements must also be taken into account when designing and operating gas

turbine cycles. For example, reducing emissions may require additional components or processes that can increase the cost and complexity of the system. Therefore, the design and operation of gas turbine cycles must consider a variety of factors to achieve the best overall performance and efficiency.

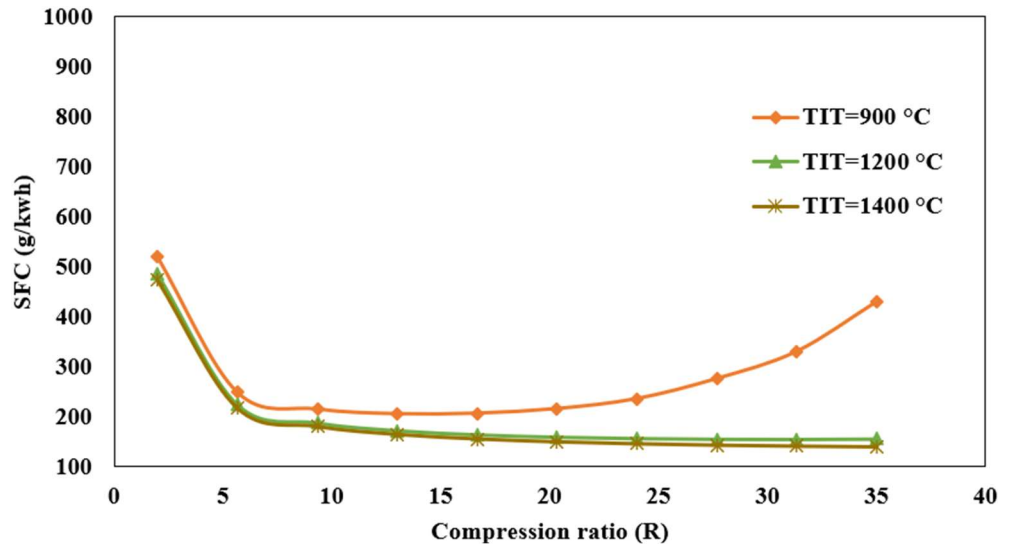


Figure 6. Specific fuel consumption variation with compression ratio and turbine inlet temperature.

3.5. Impact of compression ratio and ambient temperature on specific fuel consumption

In **Figure 7**, the SFC values are shown for gas turbine cycles operating at different pressure ratios and turbine inlet temperatures (TIT), with varying compressor inlet temperatures (T_o). The data shows that decreasing the compressor inlet temperature generally results in lower SFC values, as cooler air is denser and contains more oxygen, which can improve combustion efficiency. For example, comparing the values for TIT = 1400 °C and PR = 2, the SFC decreases from 474.2 g/kWh to 472.9 g/kWh to 471.8 g/kWh, as the T_o decrease from 35 °C to 20 °C to 5 °C, respectively. Similarly, increasing the pressure ratio can also improve fuel efficiency, as it leads to a higher turbine work output for the same amount of fuel input. For example, comparing the values for TIT = 1400 °C and $T_o = 5$ °C, the SFC decreases from 471.8 g/kWh to 135.4 g/kWh as the pressure ratio increases from 2 to 35. The data in the table also shows that there is an optimal pressure ratio that minimizes the SFC for a given TIT and T_o . This optimal value of pressure ratio generally increases as the TIT and T_o decrease. For example, for TIT = 1400 °C and $T_o = 5$ °C, the minimum SFC is achieved at PR = 35, while for TIT = 1400 °C and $T_o = 35$ °C, the minimum SFC is achieved at PR = 2. Overall, the data in the table can be used to optimize the design and operation of gas turbine cycles by selecting the appropriate TIT, T_o , and pressure ratio to achieve the desired fuel efficiency.

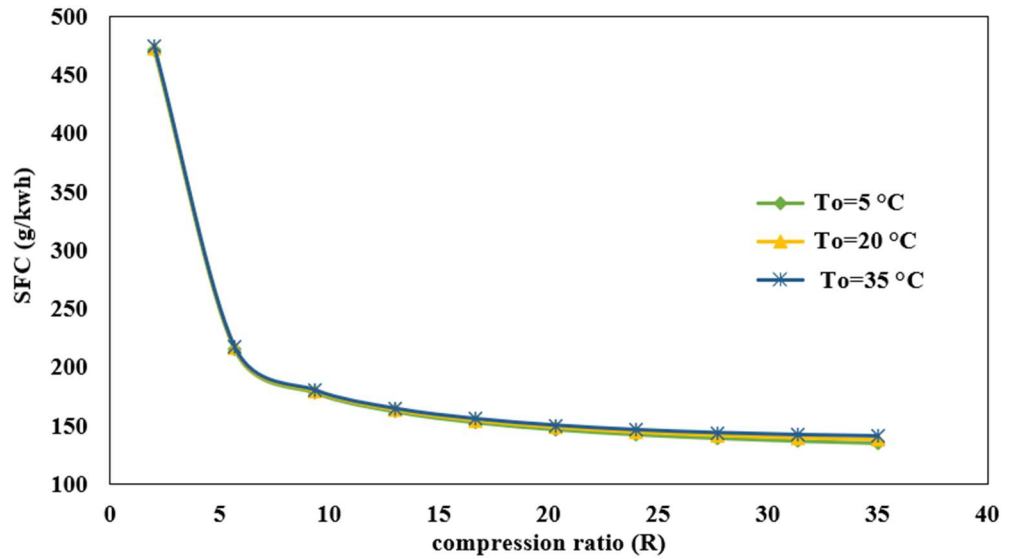


Figure 7. Specific fuel consumption variation with compression ratio and ambient temperature.

3.6. Impact of turbine inlet temperature and ambient temperature on specific fuel consumption

In **Figure 8**, the SFC values are shown for gas turbine cycles operating at different turbine inlet temperatures (TIT), with a fixed pressure ratio (R) of 20 and varying compressor inlet temperatures (T_1). The data shows that decreasing the compressor inlet temperature generally results in lower SFC values, as cooler air is denser and contains more oxygen, which can improve combustion efficiency. Similarly, increasing the turbine inlet temperature generally results in higher SFC values, as more fuel is required to maintain the higher combustion temperatures. For example, comparing the values for $T_1 = 5$ °C, the SFC increases from 190.7 g/kWh to 233.2 g/kWh, as the TIT increases from 900 °C to 1400 °C, respectively. Overall, the design and operation of gas turbine cycles must consider a variety of factors to achieve the best overall performance and efficiency. This can involve trade-offs between different factors, such as fuel efficiency, emissions, reliability, and cost, to find the optimal balance for a given application.

Table 4 provides data on the overall efficiency, exergy efficiency, and specific fuel consumption (SFC) for different combinations of turbine inlet temperature (TIT), compressor inlet temperature (T_0), and pressure ratio (R_c) for a simple gas turbine cycle. The TIT values considered are 900 °C, 1200 °C, and 1400 °C, while the T_0 values are 5 °C, 25 °C, and 35 °C, and the R_c values are 8, 20, and 30. For each combination, the table reports the energy efficiency, exergy efficiency, and SFC of the simple gas turbine cycle. Based on the data in the table, it can be observed that increasing the TIT generally leads to higher efficiency and lower SFC. Also, increasing the T_0 or R_c generally results in lower efficiency and higher SFC. For example, for TIT = 1400 °C, $T_0 = 20$ °C, and $R_c = 8$, the energy efficiency is 32.75%, the exergy efficiency is 30.9%, and the SFC is 187.9 g/kWh. However, for TIT = 900 °C, $T_0 = 30$ °C, and $R_c = 30$, the energy efficiency is only 13.18%, the exergy efficiency is 12.44%, and the SFC is 570.3 g/kWh. By analyzing the data in **Table 4**, it is possible to determine the optimal values of TIT, T_0 , and R_c for a given gas turbine

application. For example, a designer might choose a higher TIT to increase efficiency, but there may be practical limitations on the materials and technology available to achieve a high enough TIT. Similarly, a designer might choose a lower T_o to improve efficiency, but this could also reduce the power output of the gas turbine. In summary, **Table 4** provides important data for understanding the performance of simple gas turbine cycles and can be used to optimize the design of gas turbine systems for various applications.

Table 4. Overall efficiency and SFC for different values of TIT, T_o , and R_c associated with the simple gas turbine cycles.

TIT (°C)	T_o (°C)	R_c	Energy efficiency (%)	Exergy efficiency (%)	SFC (g/kwh)
900	5	8	27.77	26.2	215.5
		20	27.71	26.14	190.7
		30	21.82	20.58	215.6
	25	8	26.44	24.94	221.7
		20	23.38	22.06	213.8
		30	13.18	12.44	324.7
	35	8	25.69	24.24	225.6
		20	20.75	19.57	233.2
		30	7.426	7.006	570.3
1200	5	8	31.47	29.69	194.4
		20	36.83	34.74	155.3
		30	36.82	34.74	148
	25	8	30.75	29.01	196.4
		20	35.04	33.06	159.2
		30	34	32.08	154.5
	35	8	30.37	28.65	197.6
		20	34.04	32.11	161.7
		30	32.36	30.52	159
1400	5	8	32.75	30.9	187.9
		20	39.62	37.38	147.4
		30	40.9	38.59	138
	25	8	32.22	30.39	189.1
		20	38.4	36.23	149.5
		30	39.1	36.88	141
	35	8	31.93	30.12	189.8
		20	37.73	35.59	150.7
		30	38.08	35.92	142.8

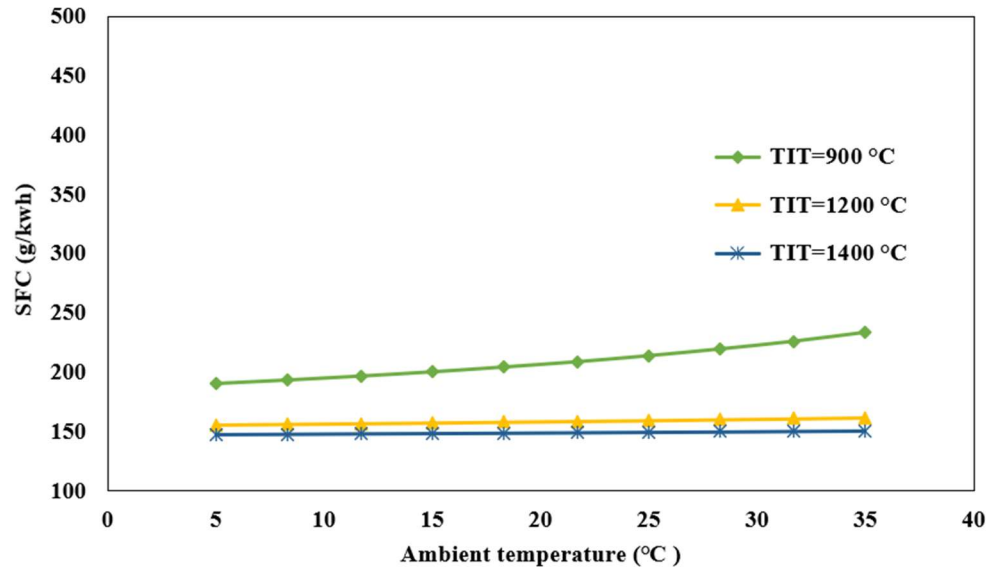


Figure 8. Illustrates how specific fuel consumption vary with ambient temperature and turbine inlet temperature.

4. Conclusion

In conclusion, the research demonstrates that turbine inlet temperature and compression ratio are important factors influencing the energy efficiency, exergy efficiency, and fuel consumption of gas turbine cycles. Higher turbine inlet temperatures and compression ratios lead to higher energy and exergy efficiencies but also higher fuel consumption. The ambient temperature also affects the performance, with cooler ambient temperatures improving efficiency up to a certain point. However, real-world gas turbine designs and operations must consider a range of factors and trade-offs. Higher turbine inlet temperatures and compression ratios enable gas turbines to operate closer to ideal Carnot cycle efficiencies. However, material constraints limit how high the inlet temperatures and pressures can go with current technology. Ambient temperatures affect the gas turbine cycle performance due to their impact on the density and mass flow rate of the inlet air. Cooler air is denser and contains more oxygen, enabling improved combustion and higher power output. However, ambient temperatures also limit how low the inlet temperatures can feasibly go.

Exergy efficiency represents the practical conversion efficiency that accounts for irreversibilities and losses in real systems. The exergy efficiencies were consistently lower than the energy efficiencies, indicating significant losses in the gas turbine cycles. In practice, gas turbine designers must consider trade-offs between efficiency gains, material constraints, durability, environmental factors, and lifecycle costs. Achieving the highest theoretical efficiencies may not translate to the optimal real-world design for a given application. There are opportunities to improve gas turbine efficiencies through innovations, including new materials, combustion enhancements, and advanced engine architectures. Higher efficiency usually comes at the cost of greater complexity, higher capital costs, material constraints, and reduced durability. Gas turbine cycles must therefore optimize a variety of parameters to achieve the best balance of efficiency, emissions, cost, and performance for the specific application.

While improving one factor may seem promising from an analysis of theoretical performance data, other practical limitations and considerations often come into play in real-world gas turbine systems.

Recommendations for future work

- A sensitivity analysis evaluates how the results may change under different conditions or assumptions. For example, determine how sensitive the efficiencies are to small changes in TIT around the optimal value. See how the results vary for different types of fuels or for part-load operation. A robust analysis considers a range of possible scenarios.
- Discuss techno-economic implications, including how the capital and operating costs of gas turbines are influenced by parameters like TIT, T_o , and R_c . Improving performance through higher temperatures and pressure ratios, for example, also tends to increase costs. The costs associated with emissions control systems can also be significant. Discuss the costs and benefits of different optimization strategies.
- Consider alternative optimization objectives, such as minimizing emissions (e.g., NOx) rather than maximizing efficiency. Determine how parameters like TIT, T_o , and R_c would differ to optimize for minimal NOx emissions and evaluate the trade-offs with efficiency. Multi-objective optimization is important for sustainability.
- Discuss opportunities for future research on next-generation gas turbines, including technologies like intercooling, recuperators, and direct firing. Speculate on new approaches that could significantly improve gas turbine performance beyond incremental changes to TIT, T_o , and R_c alone. This helps to paint a picture of the future for continued progress.

Author contributions: Conceptualization, ME and HAM; methodology, ME; software, ME; validation, ME; formal analysis, ME; investigation, AMN; resources, XX; data curation, XX; writing—original draft preparation, ME; writing—review and editing, ME, and HAM, and MRA; visualization, MRA; supervision, HAM; project administration, AMN. All authors have read and agreed to the published version of the manuscript.

Conflict of interest: The authors declare no conflict of interest.

Nomenclature

Symbols	Subscripts	Abbreviation
C_p Specific heat (KJ/kg)	a Air	AF Air to fuel ratio
h Specific enthalpy (J/kg)	c Compressor	CIT Compressor inlet temperature
m Mass flow rate (kg/s)	cc Combustion chamber	LHV Fuel heating value (kJ/kg)
P Pressure (kPa)	GT Gas turbine	NG Natural gas
q Heat supplied (W)	net Net	SGT Simple gas turbine
R_c Pressure ratio	o Outlet	SFC Specific fuel consumption (g/kwh)
s Specific entropy (J/kg K)	p Pump	TIT Turbine inlet temperature (k)

T Temperature (K)
W Work (W)

Greek symbols

η Thermal efficiency
 γ Ratio of specific heat

References

1. Liu X, Zeng Z, Hu G, Asgari A. Thermodynamic, environmental, and economic analysis of a novel power and water production system driven by gas turbine cycle. *Alexandria Engineering Journal*. 2022; 61: 9529–9551. doi: 10.1016/j.aej.2022.03.038
2. Sinha AA, Sanjay, Ansari MZ, et al. Thermodynamic assessment of biomass-fueled solid oxide fuel cell integrated gas turbine hybrid configuration. *Sustainable Energy Technologies and Assessments*. 2023; 57: 103242. doi: 10.1016/j.seta.2023.103242
3. Shabruhi Mishamandani A, Mojaddam M, Mohseni A. Integrating machine learning and thermodynamic modeling for performance prediction and optimization of supercritical CO₂ and gas turbine combined power systems. *Thermal Science and Engineering Progress*. 2024; 54: 102820. doi: 10.1016/j.tsep.2024.102820
4. da Silva JAM, Ávila Filho S, Carvalho M. Assessment of energy and exergy efficiencies in steam generators. *Journal of the Brazilian Society of Mechanical Sciences and Engineering*. 2017; 39: 3217–3226. doi: 10.1007/s40430-016-0704-6
5. Ibrahim TK, Mohammed MK, Awad OI, et al. A comprehensive review on the exergy analysis of combined cycle power plants. *Renewable and Sustainable Energy Reviews*. 2018; 90: 835–50. doi: 10.1016/j.rser.2018.03.072
6. Elwardany M, Nassib AM, Mohamed HA, Abdelaal M. Energy and exergy assessment of 750 MW combined cycle power plant: A case study. *Energy Nexus*. 2023; 12: 100251. doi: 10.1016/j.nexus.2023.100251
7. Elwardany M. Enhancing steam boiler efficiency through comprehensive energy and exergy analysis: A review. *Process Safety and Environmental Protection*. 2024; 184: 1222–50. doi: 10.1016/j.psep.2024.01.102
8. Pashchenko D, Mustafin R, Karpilov I. Ammonia-fired chemically recuperated gas turbine: Thermodynamic analysis of cycle and recuperation system. *Energy*. 2022; 252. doi: 10.1016/j.energy.2022.124081
9. Bartnik R, Hnydiuk-Stefan A, Buryń Z. Thermodynamic and economic analysis of a gas turbine set coupled with a turboexpander in a hierarchical gas-gas system. *Energy*. 2020; 190. doi: 10.1016/j.energy.2019.116394
10. Kim JS, Kim DY, Kim YT. Thermodynamic analysis of a dual loop cycle coupled with a marine gas turbine for waste heat recovery system using low global warming potential working fluids. *Journal of Mechanical Science and Technology*. 2019; 33: 3531–41. doi: 10.1007/s12206-019-0647-9
11. Shakib SE, Amidpour M, Esmaili A, et al. Various approaches to thermodynamic optimization of a hybrid multi-effect evaporation with thermal vapour compression and reverse osmosis desalination system integrated to a gas turbine power plant. *International Journal of Engineering, Transactions B: Applications*. 2019; 32: 777–89. doi: 10.5829/ije.2019.32.05b.20
12. Khosravi H, Salehi G, Azad MT. Optimization and advance thermodynamic analysis of dual stage Co₂ power cycle combined to gas turbine. *Heat and Mass Transfer/Waerme-Und Stoffuebertragung*. 2020; 56: 75–94. doi: 10.1007/s00231-019-02688-w
13. Balku S. Analysis of combined cycle efficiency by simulation and optimization. *Energy Conversion and Management*. 2017; 148: 174–83. doi: 10.1016/j.enconman.2017.05.032
14. Elwardany M, Nassib AM, Mohamed HA. Analyzing global research trends in combined cycle power plants: A bibliometric study. *Energy Nexus*. 2024; 13: 100265. doi: 10.1016/j.nexus.2023.100265
15. Park Y, Choi M, Choi G. Thermodynamic performance study of large-scale industrial gas turbine with methane/ammonia/hydrogen blended fuels. *Energy*. 2023; 282: 128731. doi: 10.1016/j.energy.2023.128731
16. Abdalla MSM, Balli O, Adali OH, et al. Thermodynamic, sustainability, environmental and damage cost analyses of jet fuel starter gas turbine engine. *Energy*. 2023; 267: 126487. doi: 10.1016/j.energy.2022.126487
17. Tianliang W, Hong T. Thermodynamic and exergoeconomic analysis of an innovative cogeneration of power and freshwater based on gas turbine cycle. *Energy*. 2023; 285: 129454. doi: 10.1016/j.energy.2023.129454
18. Jaszczur M, Dudek M, Kolenda Z. Thermodynamic analysis of advanced gas turbine combined cycle integration with a high-temperature nuclear reactor and cogeneration unit. *Energies*. 2020; 13. doi: 10.3390/en13020400
19. Golchoobian H, Taheri MH, Saedodin S. Thermodynamic analysis of turboexpander and gas turbine hybrid system for gas pressure reduction station of a power plant. *Case Studies in Thermal Engineering*. 2019; 14. doi: 10.1016/j.csite.2019.100488

20. Arsalis A. Thermodynamic modeling and parametric study of a small-scale natural gas/hydrogen-fueled gas turbine system for decentralized applications. *Sustainable Energy Technologies and Assessments*. 2019; 36. doi: 10.1016/j.seta.2019.100560
21. Xie M, Xie Y, He Y, et al. Thermodynamic analysis and system design of the supercritical CO₂ Brayton cycle for waste heat recovery of gas turbine. *Heat Transfer Research*. 2020; 51: 129–46. doi: 10.1615/HeatTransRes.2019028447
22. Stathopoulos P, Rähse T, Vinkeloe J, Djordjevic N. First law thermodynamic analysis of the recuperated humphrey cycle for gas turbines with pressure gain combustion. *Energy*. 2020; 200. doi: 10.1016/j.energy.2020.117492
23. Pirkandi J, Penhani H, Maroufi A. Thermodynamic analysis of the performance of a hybrid system consisting of steam turbine, gas turbine and solid oxide fuel cell (SOFC-GT-ST). *Energy Conversion and Management*. 2020; 213. doi: 10.1016/j.enconman.2020.112816
24. Elwardany M, Nassib AM, Mohamed HA. Case Study: Exergy Analysis of a Gas Turbine Cycle Power Plant in Hot Weather Conditions. In: *Proceedings of the 2023 5th Novel Intelligent and Leading Emerging Sciences Conference (NILES)*. pp. 291–294. doi: 10.1109/NILES59815.2023.10296731
25. Mrzljak V, Poljak I, Jelić M, Prpić-Oršić J. Thermodynamic Analysis and Improvement Potential of Helium Closed Cycle Gas Turbine Power Plant at Four Loads. *Energies*. 2023; 16. doi: 10.3390/en16155589
26. Ren J, Xu C, Qian Z, et al. Exergoeconomic Analysis and Optimization of a Biomass Integrated Gasification Combined Cycle Based on Externally Fired Gas Turbine, Steam Rankine Cycle, Organic Rankine Cycle, and Absorption Refrigeration Cycle. *Entropy*. 2024; 26. doi: 10.3390/e26060511
27. Elwardany M, Nassib AM, Mohamed HA. Exergy analysis of a gas turbine cycle power plant: a case study of power plant in Egypt. *Journal of Thermal Analysis and Calorimetry*. 2024. doi: 10.1007/s10973-024-13324-z
28. Aygun H, Caliskan H. Evaluating and modelling of thermodynamic and environmental parameters of a gas turbine engine and its components. *Journal of Cleaner Production*. 2022; 365: 132762. doi: 10.1016/j.jclepro.2022.132762
29. Skabelund BB, Jenkins CD, Stechel EB, Milcarek RJ. Thermodynamic and emission analysis of a hydrogen/methane fueled gas turbine. *Energy Conversion and Management: X*. 2023; 19: 100394. doi: 10.1016/j.ecmx.2023.100394
30. Jiang Z, Wang X, Yang S, Zhu M. A Deterministic Calibration Method for the Thermodynamic Model of Gas Turbines. *Symmetry*. 2024; 16. doi: 10.3390/sym16050522
31. Brahimi F, Madani B, Ghemmadi M. Comparative Thermodynamic Environmental and Economic Analyses of Combined Cycles Using Air and Supercritical CO₂ in the Bottoming Cycles for Power Generation by Gas Turbine Waste Heat Recovery. *Energies*. 2022; 15. doi: 10.3390/en15239066
32. Elwardany M, Nassib AEM, Mohamed HA. Comparative Evaluation for Selected Gas Turbine Cycles. *International Journal of Thermodynamics*. 2023; 26: 57–67. doi: 10.5541/ijot.1268823
33. Sammour AA, Komarov OV, Qasim MA, Saleh AY. Investigation of the Influence of Ambient Conditions on the Thermodynamic Characteristics of Air as a Working Fluid for Gas Turbines. *Journal of Advanced Research in Fluid Mechanics and Thermal Sciences*. 2023; 106: 182–96. doi: 10.37934/arfmts.106.1.182196
34. Abed AM, Chauhan BS, Ayed H, et al. Thermodynamic, exergetic and environmental evaluation and optimization of a bio-fuel fired gas turbine incorporated with wind energy derived hydrogen injection. *Case Studies in Thermal Engineering*. 2024; 56: 104238. doi: 10.1016/j.csite.2024.104238
35. Almatrafi E, Khaliq A, Abuhabaya A. Thermodynamic and exergetic assessment of a biomass derived syngas fueled gas turbine powered trigeneration system. *Case Studies in Thermal Engineering*. 2022; 35: 102099. doi: 10.1016/j.csite.2022.102099
36. Al-Tameemi MRJ, Yahya SG, Hafedh SA, Azzawi IDJ. Thermodynamic optimization of an integrated gas turbine cycle, heat exchanger and organic Rankine cycle for co-generation of mechanical power and heating load. *Journal of Computational and Applied Research in Mechanical Engineering*. 2023; 13: 75–88. doi: 10.22061/jcarme.2023.9366.2253
37. Sasmoko, Lee SW, Bhavanari M, et al. Thermodynamic Analysis of Three Internal Reforming Protonic Ceramic Fuel Cell-Gas Turbine Hybrid Systems. *Applied Sciences (Switzerland)*. 2022; 12. doi: 10.3390/app122111140
38. Alklaibi AM, Khan MN, Khan WA. Thermodynamic analysis of gas turbine with air bottoming cycle. *Energy*. 2016; 107: 603–11. doi: 10.1016/j.energy.2016.04.055
39. Elwardany M, Nassib AM, Mohamed HA, Abdelaal. Performance Assessment of Combined Cycle Power Plant. In: *Proceedings of the 2023 5th Novel Intelligent and Leading Emerging Sciences Conference (NILES)*. pp. 80–84. doi: 10.1109/NILES59815.2023.10296617
40. Ibrahim TK, Basrawi F, Awad OI, et al. Thermal performance of gas turbine power plant based on exergy analysis. *Applied*

- Thermal Engineering. 2017; 115: 977–85. doi: 10.1016/j.applthermaleng.2017.01.032
41. Kurt H, Recebli Z, Gedik E. Performance analysis of open cycle gas turbines. *International Journal of Energy Research*. 2009; 33: 285–294. doi: 10.1002/er.1472
 42. De Sa A, Al Zubaidy S. Gas turbine performance at varying ambient temperature. *Applied Thermal Engineering*. 2011; 31: 2735–9. doi: 10.1016/j.applthermaleng.2011.04.045
 43. Abou Al-Sood MM, Matrawy KK, Abdel-Rahim YM. Optimum Operating Parameters of an Irreversible Gas Turbine Cycle. *JES Journal of Engineering Sciences*. 2012; 40: 1695–714. doi: 10.21608/jesaun.2012.114611
 44. Salah SA, Abbas EF, Ali OM, et al. Evaluation of the gas turbine unit in the Kirkuk gas power plant to analyse the energy and exergy using ChemCad simulation. *International Journal of Low-Carbon Technologies*. 2022; 17: 603–10. doi: 10.1093/ijlct/ctac034
 45. Ahmadi GR, Toghraie D. Energy and exergy analysis of Montazeri Steam Power Plant in Iran. *Renewable and Sustainable Energy Reviews*. 2016; 56: 454–63. doi: 10.1016/j.rser.2015.11.074
 46. Çengel Y, Boles M. *Thermodynamics: an engineering approach*, 5th ed. McGraw-Hill Science/Engineering/Math; 2005.
 47. Ersayin E, Ozgener L. Performance analysis of combined cycle power plants: A case study. *Renewable and Sustainable Energy Reviews*. 2015; 43: 832–42. doi: 10.1016/j.rser.2014.11.082
 48. Dincer I, Rosen MA. Chemical exergy. *Exergy*. 2021; 37–60. doi: 10.1016/b978-0-12-824372-5.00003-8